Journal of Hazardous Materials 171 (2009) 378–385

Contents lists available at ScienceDirect

Journal of Hazardous Materials

journal homepage: www.elsevier.com/locate/jhazmat

Capturing 1,3-butadiene by the highly ordered Al-containing SBA-15

Ling Gao [a], Fang Na Gu [a], Yu Zhou [a], Jing Yang [a], Ying Wang [b], Jian Hua Zhu [a,*]

[a] Key Laboratory of Mesoscopic Chemistry of MOE, College of Chemistry and Chemistry Engineering, Nanjing University, 22 Hankou Road, Gu-lou, Nanjing 210093, China
[b] Ecomaterials and Renewable Energy Research Center (ERERC), Nanjing University, Nanjing 210093, China

ARTICLE INFO

Article history:
Received 7 April 2009
Received in revised form 14 May 2009
Accepted 15 May 2009
Available online 11 June 2009

Keywords:
Adsorption
1,3-Butadiene
Alumina-modified SBA-15
Environmental protection
Mesoporous materials
Volatile nitrosamines

ABSTRACT

This investigation examined the instantaneous adsorption of 1,3-butadiene by aluminum-modified mesoporous silica SBA-15 at ambient temperature. To efficiently trap the 1,3-butadiene pollutant in environment, alumina was incorporated in SBA-15 through various pathways such as one-pot synthesis, solid state grinding and impregnation, and the property–function relation of resulting composites were characterized with XRD, N_2 adsorption–desorption, FTIR and NH_3-TPD techniques. Adsorption of *N*-nitrosopyrrolidine (NPYR) was employed for the first time to reveal the difference between the mesoporous silica with the same Al-content but prepared with different methods, providing a potential method for the delicate characterization. Modification with alumina significantly increased the capability of SBA-15 to adsorb 1,3-butadiene, and the one-pot synthesized sample exhibited a higher activity than the post-modified samples, resulting from the formation of Brønsted acidic sites and reservation of silianol groups on SBA-15 host.

1. Introduction

1,3-Butadiene is a common atmospheric pollutant because it is not only a very volatile and widely used industrial chemical, but also the product of the incomplete combustion of gasoline and diesel fuels so that the significantly higher concentrations of 1,3-butadiene can be found in vehicle exposures and petrochemical companies as well as tobacco smoke [1]. It ranks 36th in the top 50 most produced chemicals within the United States [2], and is one of the top 33 in the toxic release inventory [3]. 1,3-Butadiene has been considered being carcinogenic to humans by USEPA due to its epoxide metabolites [4], because it can react with OH, O_3 and NO_3 in the atmosphere to produce a number of potentially toxic products that cause leukemia, reproductive and/or developmental toxicity [5,6]. Therefore, selective adsorption of 1,3-butadiene pollutant in the atmosphere is necessary and important for protection of public health. A challenge is to seek the new selective adsorbent materials.

Environmental purification needs to treat a large volume of gas flow fleetly to capture the trace amount of target pollutant. However, the narrow pore of zeolites related to large pressure drop therefore they fail to purify the huge mass of gas flow in aeration system within a short time. Consequently mesoporous silica became the candidate due to its large pore diameter [7], especially SBA-15 with the thick wall and high hydrothermal stability [8]. Nonetheless, the actual function of mesoporous silica in the purification of aeration system was limited since it lacked metal cation and acidic sites to provide necessary interaction towards target molecules [9]. In the current study, aluminum is chosen to modify SBA-15 because incorporation of Al into in the framework can generate bridging hydroxyl groups (SiOHAl, Brønsted acid sites) [10,11], introducing proton acidity in the mesoporous silica and promoting its performance in adsorption and catalysis. Since different preparative routes can result in the different dispersion and distribution of Al in the mesoporous silica, varying the mesostructures and textual properties of the modified composites [12–14], both one-pot synthesis and post-modification are utilized in the present study to prepare the Al-containing composite, in order to explore how the delicate morphology, say, the micropore and the tiny defect formed in the channel wall [15], and the guest metal cations of SBA-15 affect the final adsorption of 1,3-butadiene.

The dependence of 1,3-butadiene adsorption on the surface state of adsorbent was observed on the metal-modified porous materials [16–18]. 1,3-Butadiene was poorly adsorbed on the aminopropylsilyl-modified amorphous silica regardless of physical topography, because the polar surface went against the adsorption of non-polar molecule [19]. On the other hand, the olefinic double bond of 1,3-butadiene had a special interaction with the cage cation of zeolite such as Na^+ of zeolite NaX [20], and the oligomerization of 1,3-butadiene occurred on Brønsted acid sites in the acidic FAU zeolite to yield oligomeric residues containing polyalkene species [21]. On the Ag/α-Al_2O_3 catalysts 1,3-butadiene adsorbed on the positively charged Ag atoms via a single C=C bond or both C=C bonds depending on the temperature of adsorption [22]. The FTIR method

* Corresponding author. Tel.: +86 25 83595848; fax: +86 25 83317761.
E-mail address: jhzhu@nju.edu.cn (J.H. Zhu).

0304-3894/$ – see front matter © 2009 Elsevier B.V. All rights reserved.
doi:10.1016/j.jhazmat.2009.05.143

plus the new technique such as ultra-rapid-scanning or in situ diffuse reflectance was extensively used to investigate the adsorption mechanism of 1,3-butadiene [19–21]. However, the samples contacted with 1,3-butadiene statically or continually in these literatures, which cannot depict the adsorptive behavior of a composite in real applications. The concentration of 1,3-butadiene in tobacco smoke or an aeration system is variational, and the adsorbent positioned in a cigarette filter or aeration has a very short contact time with the target compounds, for example the adsorbent placed in cigarette filter only had the time less than 0.1 s to contact the harmful components under the standard cigarette-smoking test conditions [23]. Moreover, intermittent adsorption instead of continues adsorption is predominant in many potential applications. For these reasons, an instantaneous rather than steady adsorption method should be adopted to critically examine the adsorption of 1,3-butadienen in the gas stream so that we utilize a new test method, similar to concentration pulse chromatography [24], to study the adsorption of 1,3-butadiene on these Al-containing mesoporous composites.

In this paper, Al-containing SBA-15 was synthesized by the one-pot synthesis along with various post-modifications, and the textural properties of all resulting samples were characterized by powder X-ray diffraction (XRD), N_2 sorption isotherms and FTIR. Temperature programmed desorption (TPD) of ammonia was employed to assess the accessibility of newly formed acid sites in Al-containing SBA-15. To explore whether the synergy between the guest species and the silanol groups of host occurs to trap target in the metal oxide-modified SBA-15 [9], instantaneous adsorption of volatile nitrosamine *N*-nitrosopyrrolidine (NPYR) is employed as a probe measurement for the first time.

2. Experimental

2.1. Chemicals

The triblock poly(ethyleneoxide)–poly(propylene oxide)–poly(ethyleneoxide) copolymer Pluronic P123 (M_{av} = 5800, $EO_{20}PO_{70}EO_{20}$) was the product of Aldrich. Tetraethyl orthosilicate (TEOS) and hydrochloric acid were obtained from Shanghai Chemical Reagent Company (China), and all chemicals were used as received without further purification. NPYR was purchased from Sigma, and dissolved in dichloromethane at volume ratio of 1:19 and stored at 273 K [23]. Aluminum nitrate and other metal nitrate salts were A.R. grade agents. Nitrogen (99.99%) and hydrogen (99.999%) were used as the carrier gas. 1,3-butadiene (99.95%) was purchased from Nanjing Specific gas factory.

2.2. Synthesis and modification of SBA-15 sample

SBA-15 was synthesized according to literature [8]. In a typical synthesis, 4.0 g of P123 copolymer was dissolved in 150 g of 1.6 M HCl, followed by addition of 8.50 g TEOS at 313 K. The resulting mixture was stirred for 24 h and then placed in an oven at 373 K for 24 h under static condition. After the siliceous product was filtered, washed and dried, one part was calcined at 823 K in air for 5 h to get the template-free sample named as SBA-15, while the another part containing the template micelles was named as SBA-15(as).

To introduce aluminum guest into the SBA-15 host through post-modification, two methods, grinding and impregnation, were utilized. In the solvent-free modification, 0.6 g of SBA-15(as) was ground thoroughly with 170 mg of $Al(NO_3)_3{\cdot}9H_2O$ in mortar at room temperature for about 0.5 h, to get the composite with the Si/Al ratio of 10. Alternatively, 0.6 g template-free SBA-15 was manually ground with 340 mg $Al(NO_3)_3{\cdot}9H_2O$. These two resulting samples were calcined at 823 K in air for 5 h and denoted as 10AS(as-g) and 10AS(g) respectively. For impregnation, 0.6 g of template-free SBA-15 was stirred in 20 mL solution containing 340 mg $Al(NO_3)_3{\cdot}9H_2O$ at 353 K until the solvent was slowly evaporated. Finally this composite was calcined at 823 K for 5 h to get the sample named as 10AS(imp).

2.2.1. One-pot synthesis of metal-containing SBA-15

In a typical synthesis, 2 g triblock copolymer P123 and a calculated amount of metal nitrate were dissolved in 60 g 2 M HCl and 15 g H_2O, then 4.25 g TEOS was added while stirring at 313 K. The solution was stirred for 24 h at 313 K and transferred into a Teflon bottle and heated at 373 K for 24 h without stirring. After then, the solvent was then evaporated with stirring at 353 K, and the solid was dried and calcined at 823 K for 5 h to remove the template, giving the samples of AlSBA-15, CuSBA-15, FeSBA-15, ZnSBA-15, and ZrSBA-15. All of these samples had the same surface concentration of metal cation, 0.68 μmol m^{-2}. Similar procedure was used to synthesize the samples of SBA-15 modified with different amount of aluminum. The molar composition of $TEOS/P123/Al(NO_3)_3{\cdot}9H_2O/HCl/H_2O$ mixture was 1:0.02:*X*:6:192, when *X* was adjusted to 0.012, 0.024, 0.036, 0.062, 0.088, and 0.131 for the sample AS*n* with the Si/Al ratio of 80, 40, 28, 16, 10, 7, respectively.

2.3. Characterization

X-ray diffraction (XRD) patterns of sample were recorded on a set of D/MAX-RA X-ray diffractometer with Cu Kα radiation in which the X-ray tube was operated at 40 kV and 100 mA, over the 2θ range from 0.5° to 5° or from 5° to 80°. The N_2 adsorption and desorption isotherms at 77 K were measured using a Micromeritics ASAP 2020 system, in which the samples were outgassed at 573 K for 4 h prior to testing. The Brunauer–Emmett–Teller (BET) specific surface area of sample was calculated using adsorption data in the relative pressure range from 0.04 to 0.2, and the total pore volumes were determined from the amount adsorbed at a relative pressure of about 0.99. The pore size distribution curves were calculated from the analysis of the adsorption branch of the isotherm, using the Barret–Joyner–Halenda (BJH) algorithm. Conventional FTIR test was performed on a set of BRUKER 22 FTIR spectrometer with the tablet of sample and KBr. Aluminum content of sample was measured by inductive coupled plasma-atomic emission spectrometry (ICP-AES).

Temperature-programmed desorption of ammonia (NH_3-TPD) was performed in a conventional flow-type micro-reactor [25]. Instantaneous adsorption of nitrosamines was carried out by gas chromatography (GC) method as reported previously [23]. Adsorption of 1,3-butadiene was performed in a "U"-shape quartz tube reactor with a 6 mm inner diameter. 100 mg sample (20–40 meshes) was dehydrated at 823 K for 2 h in a nitrogen flow at first, and then cooled to room temperature prior to adsorption. 1,3-Butadiene was pulse injected into the reactor, 200 μL each time while the flow rate of nitrogen kept 20 mL min^{-1} so the contact time between the sample and the adsorbate was about 0.1 s [23]. The amount of residual 1,3-butadiene in gaseous effluent was detected by the "on line" Varian 3380 gas chromatography with a flame ionization detector. The injection–adsorption was repeated for several times until the sample could not significantly adsorb the 1,3-butadiene in gas stream.

3. Results and discussion

3.1. Characterization of the modified adsorbents

Fig. 1 illustrates the low-angle XRD patterns of AS*n* samples. All samples had the well-resolved patterns with a sharp peak at 0.9°

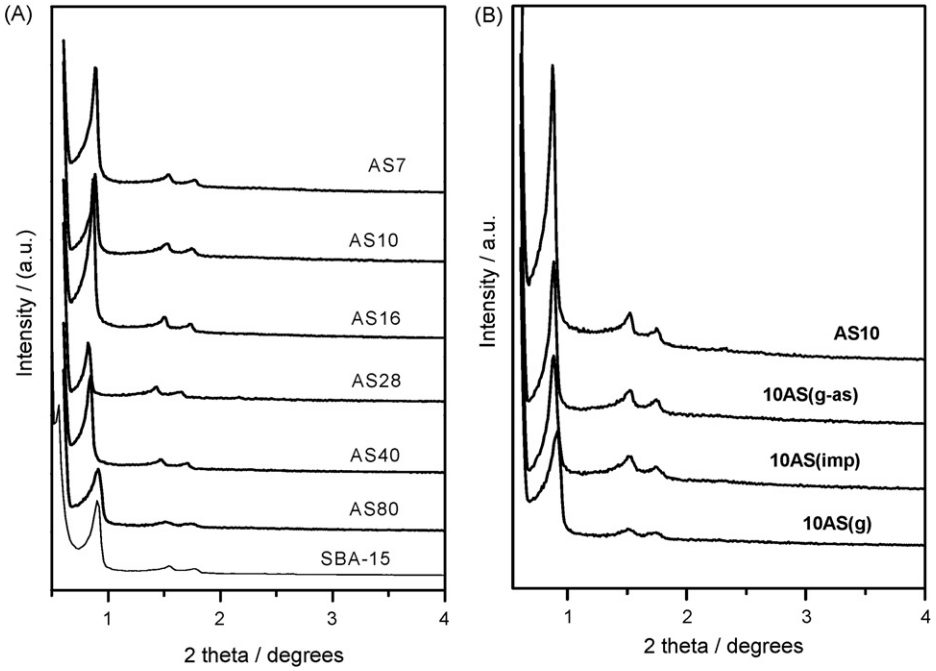

Fig. 1. Low-angle XRD patterns of Al-containing mesoporous silica (A) AS*n* and (B) 10AS samples.

and two weak ones near 1.6° and 1.8° corresponding to (1 0 0), (1 1 0) and (2 0 0) reflections (Fig. 1A) that matched well with the *p*6*mm* hexagonal symmetry [18]. The unit cell parameter of AS*n* samples, a_0 were slightly larger than that of SBA-15 as the aluminum content rose (Table 1), resulting from the incorporation of aluminum in framework due to the longer Al–O bond length than Si–O bond [26]. On the other hand, among four samples with the same Si/Al ratio of 10 but prepared in different procedures (Fig. 1B), AS10 had the strongest density of (1 0 0), (1 1 0) and (2 0 0) reflections while 10AS(g) had the weakest XRD peaks. No diffraction peak of alumina was found on the high-angle XRD patterns of four samples (Fig. 2A), meaning the well dispersion of alumina in these composites.

Fig. 3A and B exhibits the nitrogen adsorption–desorption isotherms of SBA-15 and its Al-containing analogues. AS*n* samples had the N_2 adsorption isotherms of type IV with a H1 hysteresis loop (Fig. 3A), similar to SBA-15, but a slight reduction in the N_2 adsorption capacity was observed on AS7. All isotherms exhibited a sharp step characteristic of capillary condensation of nitrogen within uniform mesopores at the higher relative pressure ($P/P_0 > 0.6$). For the sample 10AS(g), 10AS(g-as) and 10AS(imp), the sharpness of isotherms was reduced more or less while the hysteresis loop shifted towards lower P/P_0 values over a larger P/P_0 range (Fig. 3B), owing to the disadvantage of post-modification damaging the uniform mesostructures [14].

AS*n* sample possesses the average pore size slightly larger than SBA-15 (Table 1). Also, most AS*n* samples had the primary pore in the range of 6.54–6.68 nm (Fig. 3C), larger than SBA-15, with the exception of AS7 sample (6.29 nm). These phenomena originated from insertion of aluminum in framework of SBA-15 [26] because Al–O bond was longer than Si–O bond. On the other hand, the primary pore size of 10AS(g), 10AS(g-as) and 10AS(imp) changed dramatically in the range of 7.34–8.91 nm (Fig. 3D), widened than that of SBA-15, because some small pores were obstructed by alumina. Both AS*n* and the post-modified composites had the smaller surface area and pore volume than SBA-15 (Table 1).

Table 1
Structural parameters and adsorption capability of various AlSBA-15 samples.

Samples	SBA-15	AS80	AS40	AS28	AS16	AS10	AS7	10AS(g-as)	10AS(g)	10AS(imp)
Al-content (mmol g^{-1}, A)	0	0.20	0.39	0.59	0.98	1.40	1.96	1.40	1.40	1.40
a_0 (Å)	113	113	121	124	118	114	114	116	113	116
S_{BET} (m^2 g^{-1})	902	861	820	809	755	747	723	706	653	709
S_{mic} (m^2 g^{-1})	187	145	126	118	100	91	83	71	81	78
S_{mic}/S_{BET}	0.21	0.17	0.15	0.15	0.13	0.12	0.11	0.10	0.12	0.11
V_p (cm^3 g^{-1})	1.09	1.14	1.13	1.09	1.03	1.01	0.99	0.99	0.84	0.94
V_{mic} (cm^3 g^{-1})	0.08	0.06	0.05	0.05	0.04	0.03	0.03	0.02	0.03	0.03
V_{mic}/V_p (%)	7.3	5.3	4.4	4.6	3.9	3.0	3.0	2.0	3.6	3.2
D_{pa} (nm)[a]	6.30	6.42	6.40	6.52	6.61	6.66	6.46	6.47	6.11	6.35
NH_3-TPD (mmol g^{-1}, B)	0.07	0.24	0.30	0.43	0.44	0.50	0.32	0.38	0.35	0.37
ΔB (mmol g^{-1})	–	0.17	0.23	0.36	0.37	0.43	0.25	0.31	0.28	0.30
R_{NH_3} ($\Delta B/A$)	–	0.85	0.59	0.61	0.38	0.31	0.13	0.22	0.20	0.21
Trapped NPYR[b] (mmol g^{-1}, C)	0.16	0.32	0.30	0.33	0.41	0.70	0.38	0.41	0.38	0.49
ΔC (mmol g^{-1})	–	0.16	0.14	0.17	0.25	0.54	0.22	0.25	0.22	0.33
R_{NPYR} ($\Delta C/A$)	–	0.80	0.36	0.29	0.26	0.36	0.11	0.19	0.16	0.24

[a] The pore size distribution was obtained from the adsorption isotherm branches.
[b] The amount of NPYR captured by the sample when the accumulated amount of NPYR reached 1.2 mmol g^{-1}.

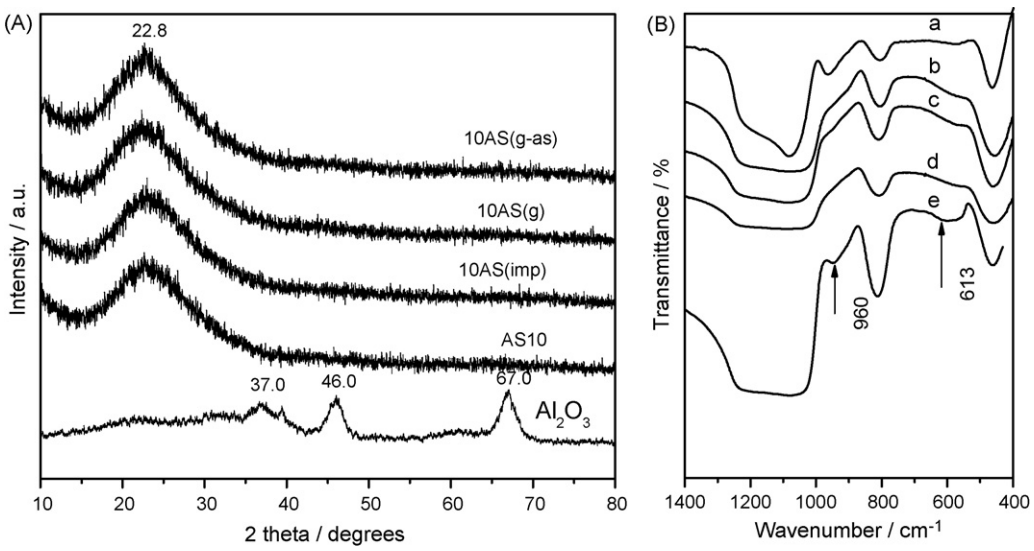

Fig. 2. High-angle XRD patterns (A) and FTIR spectra (B) of Al-containing samples (a) SBA-15, (b)10 AS(g-as), (c)10AS(imp), (d) 10AS(g) and (e) AS10.

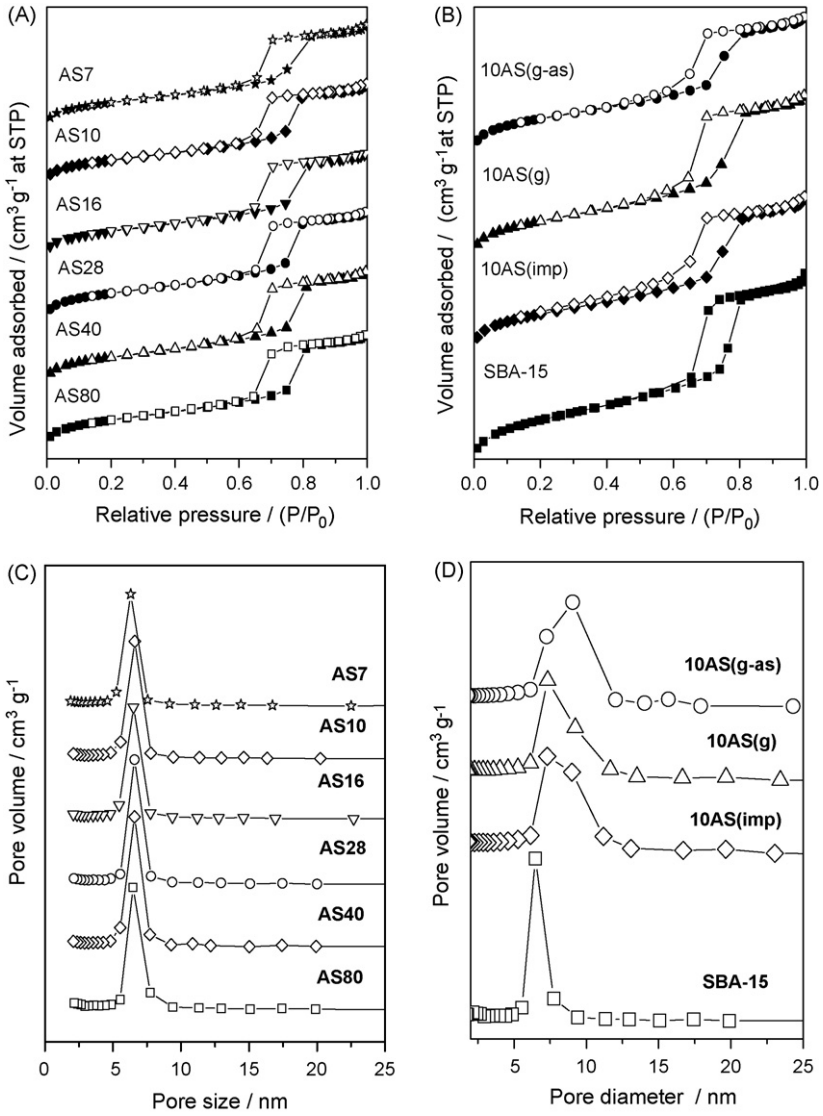

Fig. 3. N_2 adsorption–desorption isotherms (A and B) and pore size distribution (C and D) of Al-containing mesoporous samples.

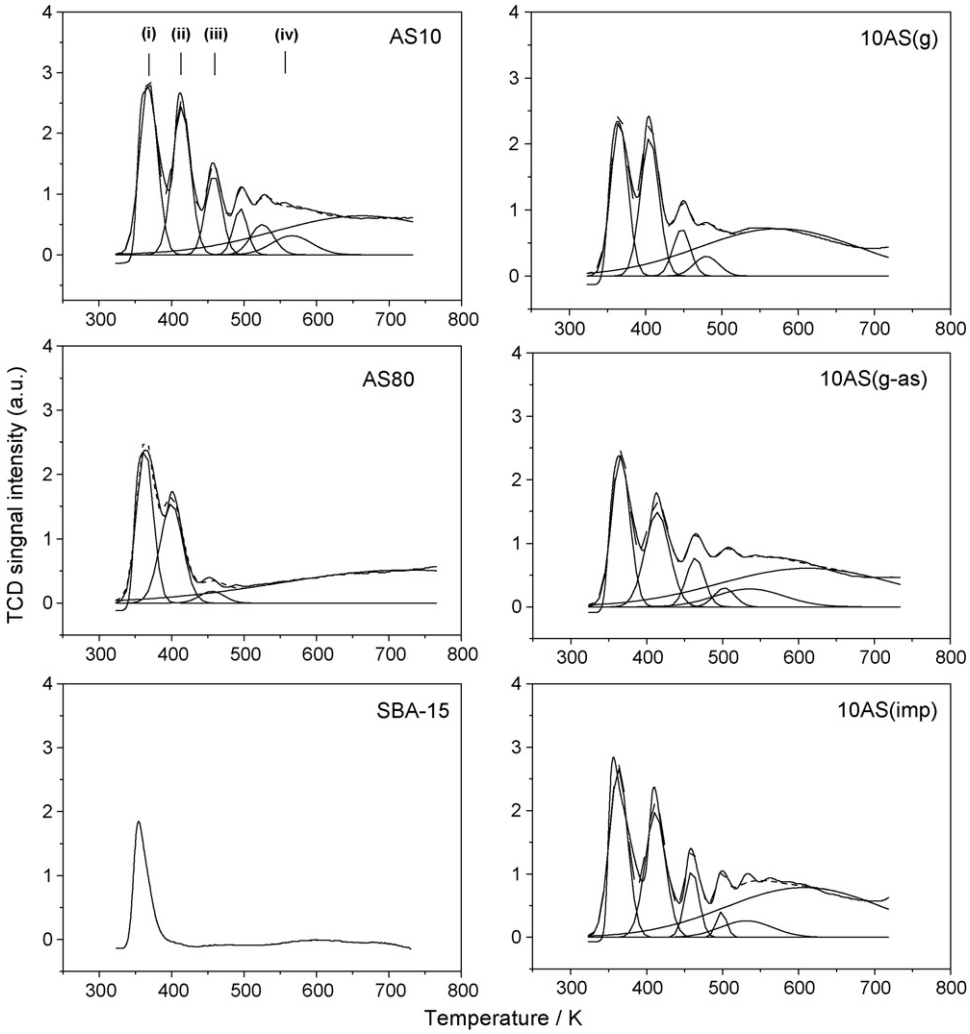

Fig. 4. NH_3-TPD curves for SBA-15 and the Al-containing SBA-15 prepared in different methods. Peaks were deconvoluted using Gaussian multi-peak fitting.

Fig. 2B describes the FTIR spectra of alumina-modified SBA-15 in the region of 400–1400 cm^{-1}. The 960 cm^{-1} band of Si–OH stretching vibration substantially decreased on the spectra of 10AS(*m*) samples because coating alumina consumed surface silanol of SBA-15 [15,9]. The 613 cm^{-1} band originated from the asymmetric vibration of condensed AlO_6 groups [27,28], and it could be assigned to structural aluminum coordinated groups, confirming the insertion of aluminum into the framework of AS10.

Fig. 4 depicts the NH_3-TPD profiles of AS10, AS80, parent SBA-15 and post-modified analogues to assess the accessibility of new-formed acidic site, in which the peak of desorbed NH_3 is deconvoluted by using Gaussian function with temperature as variant [29]. SBA-15 had only one desorption around 368 K with a small amount (0.07 mmol g^{-1}). AS10 sample possessed several more desorption peaks: peaks (ii) and (iii) near 410 K and 460 K were assigned to moderate strong Brønsted acid sites [30], the one in 480–550 K originated from strong Brønsted acidic sites owing to the presence of trivalent aluminum in different framework positions [31], and the peak (iv) around 600 K was attributed to Lewis acid sites that might arise from tricoordinated aluminum in framework [32]. With the smaller Al-content, AS80 sample showed the lower desorbed amount of NH_3 than AS10 (Table 1), confirming the relation between the newly formed acidic sites and the Al species incorporated into framework of the composite [33]. On the other hand, the amount of NH_3-desorbed in the four samples with the same Si/Al ratio of 10 increased in the order of AS10 > 10AS(imp) > 10AS(g-as) > 10AS(g), indicating the high efficiency of one-pot synthesis in creating acidic site on SBA-15. If we calculate the adsorptive efficiency of composite as the net-increased amount of NH_3 divided by the Al-content, it is clear that the highest efficiency of Al modifier, R_{NH_3}, appears on the sample of AS80 instead of AS10. AS10 contained six times more aluminum species than AS80, but trapped only double amount of NH_3 (Table 1). On the other hand, three post-modified samples had the lower adsorptive efficiency than AS10.

3.2. Trapping volatile nitrosamine in airflow

Fig. 5 describes the adsorption of NPYR in gas stream by SBA-15 and its Al-containing analogues at 453 K. All Al-containing samples had a higher capability than SBA-15 to capture the carcinogen, and among them AS10 was the best one. When the accumulated amount of NPYR reached 1.2 mmol/g, AS80 could adsorb double amount of NPYR in comparison with parent SBA-15 (Table 1), AS16 trapped 41% of the adsorbate while AS10 captured 70%. Three post-modified samples showed a lower ability than AS10 in the adsorption as shown in Fig. 6. For an overall analysis of the adsorption isotherms, we tried to fit the experimental isotherms by Freundlich adsorption equation [34],

$$\ln q = \ln K_F + \frac{1}{n} \times \ln C,$$

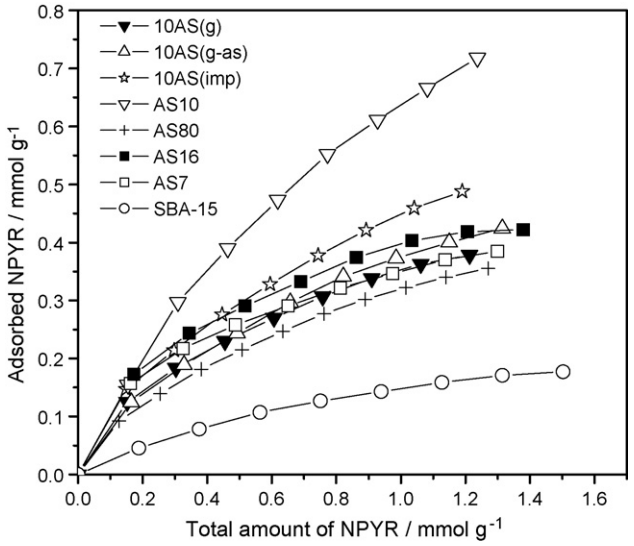

Fig. 5. Adsorption of NPYR in gas stream by Al-containing mesoporous silica at 453 K.

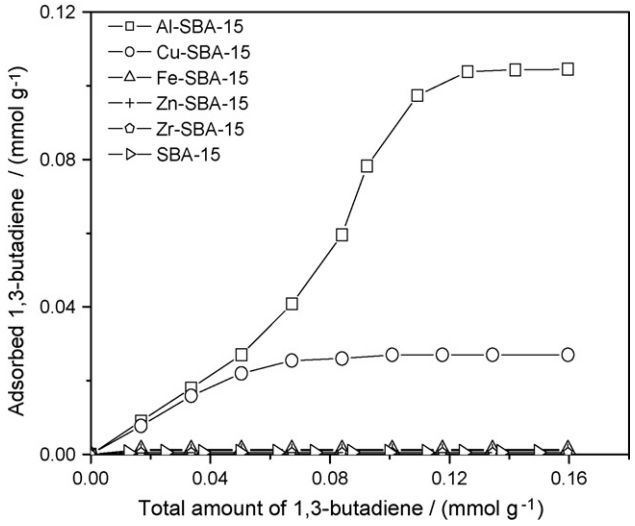

Fig. 6. . Adsorption of 1,3-butadiene on different mental oxide functionalized SBA-15 samples.

and Table 2 lists the isotherm parameters calculated with the method of least squares. For these samples, the exponent of $1 < n < 10$ indicates the favorable nature of adsorbent-NPYR system. The K_F value of NPYR in AS10, which is related to the adsorbent capacity, was about three times larger than that in SBA-15, originating from the existence of aluminum because Al cation could provide the electrostatic interaction toward the N–NO group of nitrosamine to promote the adsorption of nitrosamines in the adsorbent [25]. The smallest value of n was also observed on AS10.

Table 2
Freundlich constants of the adsorption isotherms of NPYR in Al-containing SBA-15 samples.

Samples	K_f	n	R^2
SBA-15	0.15	1.52	0.99
AS80	0.32	1.64	1.00
AS10	0.65	1.38	0.99
AS(imp)	0.45	1.70	1.00
AS(g)	0.37	1.66	0.99
AS(g-as)	0.35	1.84	1.00

Monocyclic nitrosamines such as NPYR usually take planar structure because of their large rotational barriers of the N–NO bond [35], and their N–N=O group can be attracted by the cations of adsorbent through electrostatic interaction, promoting the movement of whole molecule towards the channel of adsorbent [7,25]. Thus, incorporation of aluminum in SBA-15 is helpful for the adsorption of volatile nitrosamines. Hydrogen-bonded adsorption enables SBA-15 to weakly trap nitrosamines, and the synergy of adjacent silanol groups with the metal site in the adsorption has been reported on the copper-modified SBA-15 [9]. Such synergy may be invoked to explain the relatively higher adsorptive capability of AS10(imp) than AS10(g) or AS10(g-as), because the surface silanol groups interacted with the guest species and can be depleted in the solvent-free method while some silanol groups contacted with the solvent during the impregnation process so that they can be recovered after drying the sample [36]. However, we had no strong experimental evidence to back up this conjecture since the difference between the 960–990 cm^{-1} band of three post-modified samples, that is given by the surface silanol groups (≡Si–OH) stretching modes, in the IR spectra was not obvious (Fig. 2B).

Table 1 lists the adsorptive efficiency of composites toward NPYR. AS80 was still the champion and the R_{NPYR} of AS*n* sample declined as the Al-content increased with the exception of AS10 that was the runner-up. Also, AS10 had the value of R_{NPYR} higher than the three post-modified samples. These composites had three different behaviors in adsorption of ammonia and NPYR. A majority of the Al-containing composites showed a similar adsorptive capacity in two tests within the experimental error of ±10%, whereas AS10, AS80 and 10AS(imp) exhibited a slightly higher activity in the adsorption of NPYR. SBA-15 had a weak ability to trap ammonia but adsorbed more NPYR (Table 1) because of the function of surface silianol group [9]. Contrarily, AS28 trapped 23% less NPYR than ammonia (Table 1), resulting probably from the inaccessibility of some acidic sites due to the space hindrance.

3.3. Adsorption of 1,3-butadiene by Al-containing SBA-15

Fig. 6 delineates the instantaneous adsorption of 1,3-butadiene by the SBA-15 one-pot synthesized with various metal compounds. Incorporation of Fe, Zn or Zr did not activate SBA-15 in the adsorption, while Cu-SBA-15 could trap 1,3-butadiene but its capacity was saturated at 0.027 mmol g^{-1}. A significant promotion was observed on Al-SBA-15 that adsorbed the 1,3-butadiene of 0.104 mmol g^{-1}, three times more than that by Cu-SBA-15 at the same conditions, consequently aluminum was chosen as the modifier for further investigation.

Fig. 7 shows the adsorption of 1,3-butadiene on the SAB-15 containing different amount of aluminum. The adsorption capability of Al-SBA-15 increased as its Al-content rose, achieving the maximum in the case of AS10 since AS7 sample trapped less 1,3-butadiene (Fig. 7A). The sample with low Al-content such as AS80 and AS40 quickly lost its adsorptive ability once the accumulated amount of 1,3-butadiene achieved 0.1 mmol g^{-1}, but AS10 kept its activity until the amount of 1,3-butadiene reached 0.25 mmol g^{-1}. It is find that the capacity of sample in adsorbing 1,3-butadiene is proportional to the desorption amount of ammonia in TPD test, but not coinciding wholly with its capability in the adsorption of NPYR.

A strange phenomenon appears in Fig. 7B in which three post-modified Al-containing SBA-15 exhibit different activity in adsorbing 1,3-butadiene. Both 10AS(g) and 10AS(g-as) samples had a very weak capability and they only captured 0.006 and 0.003 mmol g^{-1} of 1,3-butadiene in the instantaneous adsorption. 10AS(imp) could trap the 1,3-butadiene of 0.09 mmol g^{-1} under the same conditions, but much inferior to AS10 whose adsorptive capacity reached 0.17 mmol g^{-1}. These four samples exhibited similar difference in the adsorption of NPYR (Fig. 5), but the difference

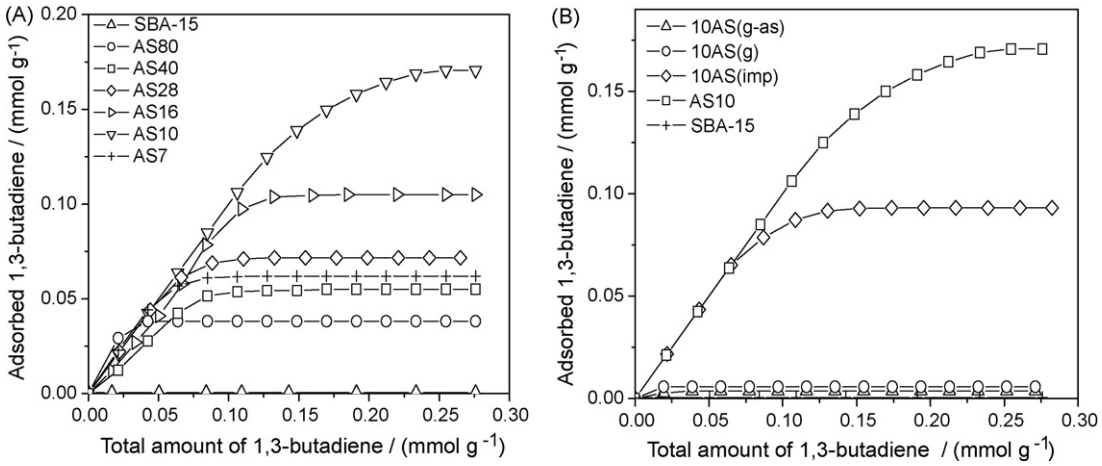

Fig. 7. Adsorption of 1,3-butadiene on AlSBA-15 samples (A) one-pot synthesized and (B) post-modified.

is dramatically magnified here. This is the first time to find so obvious difference in adsorption experiment between the mesoporous silica with the same Al-content but prepared with different methods, providing a potential method for the delicate characterization. However, this distinct difference cannot be assigned to either the accessibility of Al sites or the ratio of micropore to mesopore in the composite, and further study is required.

Fig. 8 shows the FTIR spectrum of 1,3-butadiene adsorbed on AS*n* samples at 300 K. SBA-15 was inactive in the adsorption. Once the aluminum species was incorporated into SBA-15, the bands of 1,3-butadiene appeared in the spectrum and their intensity increased as the Al-content rose in the composite. The negative band at 3740 cm^{-1} indicates the loss of isolated OH groups over an octahedrally coordinated Al ion, implying the interaction between 1,3-butadiene and the OH groups [21]. Intense bands at ca. 3100 and 3000 cm^{-1} correspond to alkene CH stretching (=CH_2 and =CHR) of 1,3-butadiene. The saturated CH stretching and deformation bands (2920, 2840 and 1400–1370 cm^{-1}) together with the C=C stretching band near 1640 cm^{-1} mean the formation of *cis*- and *trans*-2-butenes interacting via π-banding with the Brønsted OH-groups of the adsorbent. The strong band around 1825–1806 cm^{-1} is an overtone of CH_2 out-of-plane deformation mode in CHR=CH_2 groups, confirming the adsorption of 1,3-butadiene in the Al-containing sample. The adsorption band near 1500 cm^{-1} is corresponding to the formation of aromatic compounds [37], and the bands around 1590 and 1400 cm^{-1} can be attributed to the respective C=C- and C–C- stretching modes in dehydrogenated carbonaceous species with an aromatic nature. These spectra imply the strong and complex interaction of 1,3-butadiene adsorbed with the Al-containing SBA-15. The acidity of Al-SBA-15 samples has a strong influence on the adsorption of 1,3-butadiene. Brønsted acid sites of Al-SBA-15 may provide the proton to interact with 1,3-butadiene, forming *cis*- and *trans*-2-butenes via π-banding. Lewis acid sites can play an important part in many catalytic processes [38], so the 1,3-butadiene molecule adsorbed in the channel of SBA-15 will be isomerized or aromatized in several consecutive reactions. Accordingly, the capacity of AS*n* sample in the adsorption of 1,3-butadiene is proportional to its total acidity (Table 1 and Fig. 7A). Aluminum is hardly incorporated into the siliceous framework of SBA-15 during the grinding procedure so the modifier mainly forms the non-framework species. This may be one reason why 10AS(g) and 10AS(g-as) samples exhibit the poor ability in adsorbing 1,3-butadiene.

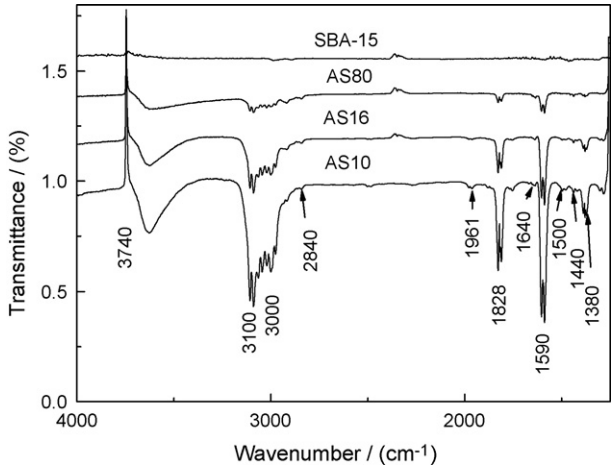

Fig. 8. FTIR spectra of 1,3-butadiene adsorbed on in situ AlSBA-15 samples at room temperature.

4. Conclusion

(1) SBA-15 is inactive in the instantaneous adsorption of 1,3-butadiene. Among various metal salt additive used in one-pot synthesis, Al has the best promotion on the adsorption of SBA-15 forward 1,3-butadiene, superior to Cu, Fe, Zn and Zr.
(2) Introducing aluminum into SBA-15 is crucial for adsorbing 1,3-butadiene. One-pot synthesis can effectively incorporate Al into the framework of SBA-15 to form Brønsted acid sites without damage of the original pore structure. Moreover, most of the surface silianol groups of SBA-15 remain, promoting the synergy with the cation in adsorption of nitrosamines or 1,3-butadiene. Post-alumination evidently lowers the surface area and pore volume of SBA-15, reducing the intensity of silianol groups.
(3) The variation in the ratio of microporous volume to mesoporous volume in the sample of Al-modified SAB-15 has the unconspicuous influence on the instantaneous adsorption of 1,3-butadiene, mirroring the minor role played by the micropore in SBA-15 in the adsorption.

This study is our first preliminary approach to develop the mesoporous functional materials for reduction of 1,3-butadiene concentration in environment. Further investigations are required to clearly identify detail characteristics of the process.

Acknowledgements

Financial support from the National Natural Science Foundation of China (20773601, 20873059 and 20871067), National Basic Research Program of China (2007CB613301), Grant 2008AA06Z327 of 863 projects, Jiangsu Provincial Natural Science Foundation Industrial Supporting Program (BE2008126), Jiangsu Province Environmental Protection Bureau Program (2008005), and Analysis Center of Nanjing University is gratefully acknowledged.

References

[1] D.E. Angove, C.J.R. Fookes, R.G. Hynes, C.K. Walters, M. Azzi, The characterisation of secondary organic aerosol formed during the photodecomposition of 1,3-butadiene in air containing nitric oxide, Atmos. Environ. 40 (2006) 4597–4607.
[2] US OSHA, Safety and Health Topics: 1,3-Butadiene, U.S. Department of Labor, Washington, DC, 2002, Available: http://www.osha.gov/SLTC/butadiene/, accessed January 2004.
[3] US EPA, Air Toxics Website, U.S. Environmental Protection Agency, Research Triangle Park, NC, 2001, Available: http://www.epa.gov/ttn/atw/urban/list33.html, accessed January 2004.
[4] US EPA, Health Assessment of 1,3-butadiene. U.S. Environmental Protection Agency Report EPA/600/P-98/001F, 2002.
[5] R.J. Srama, P. Rössner, O. Beskid, H. Bavorova, D. Ocadlikova, I. Solansky, R.J. Albertini, Chromosomal aberration frequencies determined by conventional methods: parallel increases over time in the region of a petrochemical industry and throughout the Czech Republic, Chem.-Biol. Interact. 166 (2007) 239–244.
[6] F. Pacchierotti, C. Tiveron, R. Ranaldi, B. Bassani, E. Cordelli, G.M. Leter, Reproductive toxicity of 1,3-butadiene in the mouse: cytogenetic analysis of chromosome aberrations in first-cleavage embryos and flow cytometric evaluation of spermatogonial cell killing, Mutat. Res. 397 (1998) 55–66.
[7] J.H. Zhu, S.L. Zhou, Y. Xu, Y. Cao, Y.L. Wei, Ordered mesoporous materials. Novel catalyst for degradation of N′-nitrosonornicotine, Chem. Lett. 32 (2003) 338–339.
[8] D.Y. Zhao, J. Feng, Q. Huo, N. Melosh, G.H. Fredrickson, B.F. Chmelka, G.D. Stucky, Triblock copolymer syntheses of mesoporous silica with periodic 50 to 300 Angstrom pores, Science 279 (1998) 548–552.
[9] C.F. Zhou, Y.M. Wang, Y. Cao, T.T. Zhuang, W. Huang, Y. Chun, J.H. Zhu, Solvent-free surface functionalizing SBA-15 as versatile trap of nitrosamines, J. Mater. Chem. 16 (2006) 1520–1528.
[10] Y.H. Yue, A. Gédéon, J.L. Bonardet, N. Melosh, J.B. D'Espinose, J. Fraissard, Direct synthesis of AlSBA mesoporous molecular sieves: characterization and catalytic activities, Chem. Commun. (1999) 1967–1968.
[11] L.Y. Shi, Y.M. Wang, A. Ji, L. Gao, Y. Wang, In situ direct bifunctionalization of mesoporous silica SBA-15, J. Mater. Chem. 15 (2005) 1392–1396.
[12] S. Wu, Y. Han, Y.C. Zou, J.W. Song, L. Zhao, Y. Di, S.Z. Liu, F.S. Xiao, Synthesis of heteroatom substituted SBA-15 by the "pH-Adjusting" method, Chem. Mater. 16 (2004) 486–492.
[13] M. Jang, E.W. Shin, J.W. Park, S.I. Choi, Mechanisms of arsenate adsorption by highly-ordered nano-structured silicate media impregnated with metal oxides, Environ. Sci. Technol. 37 (2003) 5062–5070.
[14] Z. Luan, M. Hartmann, D.Y. Zhao, W.Z. Zhou, L. Kevan, Alumination and ion exchange of mesoporous SBA-15 molecular sieves, Chem. Mater. 11 (1999) 1621–1627.
[15] Z.Y. Wu, H.J. Wang, T.T. Zhuang, L.B. Sun, Y.M. Wang, J.H. Zhu, Multiply functionalization of mesoporous silica in one-pot: direct synthesis of aluminum-containing plugged SBA-15 from nitrate aqueous solutions, Adv. Funct. Mater. 18 (2008) 82–94.
[16] G. Gesterberger, R. Anwander, Screening of rare earth metal grafted MCM-41 silica for asymmetric catalysis, Micropor. Mesopor. Mater. 44–45 (2001) 303–310.
[17] A. Sárkány, Zs. Révay, Some features of acetylene and 1,3-butadiene hydrogenation on Ag/SiO_2 and Ag/TiO_2 catalysts, Appl. Catal. A: Gen. 243 (2003) 347–355.
[18] M.D. Wildberger, T. Mallata, U. Golbel, A. Baiker, Oxidation of butane and butadiene to furan over vanadia-silica mixed oxides, Appl. Catal. 168 (1998) 69–80.
[19] B.A. Weinstock, H. Yang, P.R. Griffiths, Determination of the adsorption rates of aldehydes on bare and aminopropylsilyl-modified silica gels by polynomial fitting of ultra-rapid-scanning FT-IR data, Vib. Spectrosc. 35 (2004) 145–152.
[20] T. Armaroli, E. Finocchio, G. Busca, S. Rossini, A FT-IR study of the adsorption of C5 olefinic compounds on NaX zeolite, Vib. Spectrosc. 20 (1999) 85–94.
[21] T.V. Voskoboinikov, B. Coq, F. Fajula, R. Brown, G. McDougall, J.L. Couturier, An in situ diffuse reflectance FTIR study of the cyclodimerization of 1,3-butadiene over Cu-exchanged zeolites, Micropor. Mesopor. Mater. 24 (1998) 89–99.
[22] J. Müslehiddinoglu, M. Albert Vannice, Adsorption of 1,3-butadiene on supported and promoted silver catalysts, J. Catal. 222 (2004) 214–226.
[23] C.F. Zhou, Y. Cao, T.T. Zhuang, W. Huang, J.H. Zhu, Capturing volatile nitrosamines in gas stream by zeolites: why and how? J. Phys. Chem. C 111 (2007) 4347–4357.
[24] P.J.E. Harlick, F.H. Tezel, A novel solution method for interpreting binary adsorption isotherms from concentration pulse chromatography data, Adsorption 6 (2000) 293–309.
[25] Y. Cao, L.Y. Shi, Z.Y. Yun, C.F. Zhou, Y. Wang, J.H. Zhu, Novel amorphous functional materials for trapping nitrosamines, Environ. Sci. Technol. 39 (2005) 7254–7259.
[26] G. Calleja, J. Aguado, A. Carrero, J. Moreno, Preparation, characterisation and testing of Cr/AlSBA-15 ethylene polymerization catalysts, Appl. Catal. A: Gen. 316 (2007) 22–31.
[27] P. Padmaja, K.G.K. Warrier, M. Padmanabhan, W. Wunderlich, F. Berry, M. Mortimer, N.J. Creamer, Structural aspects and porosity features of nano-size high surface area alumina-silica mixed oxide catalyst generated through hybrid sol–gel route, Mater. Chem. Phys. 95 (2005) 56–61.
[28] J.M. Saniger, Al–O infrared vibrational frequencies of γ-alumina, Mater. Lett. 22 (1995) 109–113.
[29] H.G. Karge, V. Dondur, J. Weitkamp, Investigation of the distribution of acidity strength in zeolites by temperature-programmed desorption of probe molecules. 2. Dealuminated Y-type zeolites, J. Phys. Chem. 95 (1991) 283–288.
[30] M.V. Landau, E. Dafa, M.L. Kaliya, T. Sen, M. Herskowitz, Mesoporous alumina catalytic material prepared by grafting wide-pore MCM-41 with an alumina multilayer, Micropor. Mesopor. Mater. 49 (2001) 65–81.
[31] S.K. Badamali, A. Sakthivel, P. Selvam, Tertiary butylation of phenol over mesoporous H-FeMCM-41, Catal. Lett. 65 (2000) 153–157.
[32] A. Sakthivel, S.E. Dapurkar, N.M. Gupta, S.K. Kulshreshtha, P. Selvam, The influence of aluminium sources on the acidic behaviour as well as on the catalytic activity of mesoporous H-AlMCM-41 molecular sieves, Micropor. Mesopor. Mater. 65 (2003) 177–187.
[33] A. Ratnamala, V. Durgakumari, K. Lalitha, M. Subrahmanyam, Unique vapor phase synthesis of 1,2,3,5,6,7-hexahydrodicyclopenta[*b*,*e*]pyridine selectively over Co-Al-MCM-41, Catal. Commun. 8 (2007) 267–274.
[34] F.L. Slejko, Adsorption Technology: A Step-by-Step Approach to Process Evaluation and Application, Marcel Dekker, New York, 1985.
[35] M. Miura, S. Sakamoto, K. Yamaguchi, T. Ohwada, Influence of structure on N–NO bond cleavage of aliphatic *N*-nitrosamines, Tetrahedron Lett. 41 (2000) 3637–3641.
[36] Y.M. Wang, Z.Y. Wu, J.H. Zhu, Surface functionaization of SBA-15 by solvent-free method, J. Solid State Chem. 177 (2004) 3815–3823.
[37] P. Ivanov, H. Papp, In situ FT-IR study on the reaction path of skeletal isomerization of n-butene over different zeolites, Appl. Surface Sci. 179 (2001) 234–239.
[38] J.M. Du, H.L. Xu, J. Shen, J.J. Huang, W. Shen, D.Y. Zhao, Catalytic dehydrogenation and cracking of industrial dipentene over M/SBA-15 (M = Al, Zn) catalysts, Appl. Catal. A: Gen. 296 (2005) 186–193.